УДК 550.836

ГЕОТЕРМИЧЕСКОЕ ПОЛЕ ЗОНЫ ПЕРЕХОДА МЕЖДУ АНАТОЛИЙСКОЙ ПЛИТОЙ И ВОСТОЧНО-ЕВРОПЕЙСКОЙ ПЛАТФОРМОЙ

СИАМАК МАНСУРИ ФАР[1)]

[1)]*Белорусский государственный университет, пр. Независимости, 4, 220030, г. Минск, Беларусь*

В восточной части Средиземного моря выделяют обширную провинцию низкого теплового потока, простирающуюся во всем бассейне моря восточнее Крита (Левантинское море), включая Кипр и северный Египет. Геология территории восточной Анатолии сложна из-за недавней тектонической и вулканической активности. Этот регион включает главные тектонические блоки Понтийских гор, Анатолийско-Тавридский пояс и сутурную зону Битлиса, Северо- и Восточно-Анатолийский разломы. Во многих частях Анатолии встречаются офиолиты и молодые вулканические породы. Черное море окружено Альпийско-Гималайским складчатым поясом (Крым, Большой Кавказ, Понтийские горы, Родопо-Странджский массив, восточное Среднегорье, Северная Добруджа) и древними тектоническими блоками различного происхождения и возраста, такими как Восточно-Европейский кратон, Мизийская платформа, Стамбульская зона и Аджаро-Триалетская складчатая система. В Черном море преобладает низкий тепловой поток. Наименьшие значения (менее 30 мВт/м^2) зарегистрированы в центральных частях западного и восточного бассейнов Черного моря с максимальной мощностью осадочных отложений. Геотермические исследования на территории Украины ведутся в течение 45 лет. Многие особенности теплового поля остаются неизученными. Это относится, в частности, к Украинскому щиту и южной части региона Карпат. В целом территория альпийской складчатости в пределах Турции, Мраморного и Эгейского морей, Кавказа характеризуется высоким тепловым потоком. Аномалия его наибольших значений (более 100–150 мВт/м^2) отмечается на западе Турции, где преобладают тектонические условия растяжения и ведется использование подземного пара для выработки электроэнергии. Построены карта и три профиля теплового потока, пересекающих изучаемый регион.

Ключевые слова: Средиземное море; Кипр; Турция; Черное море; Украина; геотермическое поле; тепловой поток; альпийский орогенез; Большой Кавказ.

GEOTHERMAL FIELD OF THE TRANSITION AREA BETWEEN THE ANATOLIAN PLATE AND THE EAST EUROPEAN PLATFORM

SIAMAK MANSOURI FAR[a]

[a]*Belarusian State University, 4 Niezaliežnasci Avenue, Minsk 220030, Belarus*

Heat flow data from the Eastern Mediterranean region indicates an extensive province of low heat flow, spreading over the whole basin of the Mediterranean to the east of Crete (Levantine Sea), Cyprus, and Northern Egypt. Surface geology of East Anatolia is complex because of recent active tectonic and volcanic activity. The region is composed of major tectonic units of Pontides, the Anatolid-Tauride Belt and Bitlis Suture Zone, North and East Anatolian faults. Ophiolitic and young volcanic rocks can be observed in many parts of East Anatolia. The Black Sea is surrounded by the Alpine-Himalayan

Образец цитирования:
Сиамак Мансури Фар. Геотермическое поле зоны перехода между Анатолийской плитой и Восточно-Европейской платформой. *Журнал Белорусского государственного университета. География. Геология.* 2019;2:133–148.
https://doi.org/10.33581/2521-6740-2019-2-133-148

For citation:
Siamak Mansouri Far. Geothermal field of the transition area between the Anatolian Plate and the East European Platform. *Journal of the Belarusian State University. Geography and Geology.* 2019;2:133–148. Russian.
https://doi.org/10.33581/2521-6740-2019-2-133-148

Автор:
Сиамак Мансури Фар – аспирант кафедры региональной геологии факультета географии и геоинформатики. Научный руководитель – доктор геолого-минералогических наук, доцент В. И. Зуй.

Author:
Siamak Mansouri Far, postgraduate student at the department of regional geology, faculty of geography and geoinformatics.
siamak_mansourifar@yahoo.com

Orogenic Belt of Crimea, Greater Caucasus, Pontides, Rhodope-Stranja Massif, Eastern Srednegorie, North Dobrogea and older tectonic units of different origins and ages such as the Precambrian East European Craton, Moesian Platform, Istanbul Zone and Adzhar-Trialet Folded System. Low heat flow density dominates in the Black Sea. The lowest (less 30 mW/m^2) values have been recorded in central parts of the Western and Eastern Black Sea basins with maximal sedimentary thickness. Geothermal studies within the territories of Ukraine have been under way since sixties. Many important features of the thermal field remain unstudied. This applies in particular to the Ukrainian Shield and to the southern part of the Carpathian region. In general, the territory of Alpine folding within Turkey, Marmara and Aegean seas, Caucasus is characterized by high heat flow. The anomaly of its highest values (above 100–150 mW/m^2) exists within western Turkey, where tectonic conditions of extension prevail and underground steam is used to produce electricity. Three heat flow density profiles crossing the studied region and heat flow map were compiled.

Keywords: Mediterranean; Cyprus; Turkey; Black Sea; Ukraine; geothermal field; heat flow; Alpine orogeny; Greater Caucasus.

Introduction

The Anatolian Plate and the Black Sea Basin are the main tectonic units within the considered region. Given its location in the Alpine-Himalayan orogenic belt, and at the collisional boundary between Gondwana and Laurasia, the geological history of the Aegean region and Anatolia involves the Mesozoic-Cenozoic closure of several Neotethyan oceanic basins, continental collisions and subsequent post-orogenic processes [1–3]. The considered region has rather complex crustal structure.

The opening of oceanic branches of Neotethys commenced in the Triassic and closed during the Late Cretaceous to Eocene time interval. The closure of Neotethyan basins is recorded by several suture zones (e. g. Vardar, Izmir – Ankara – Erzincan, Bitlis – Zagros, Intrapontide, Antalya sutures), along which Jurassic-Cretaceous ophiolites and melanges exposed. The polarity of subduction, the timing of ocean basin opening and closure, and the location of Neotethyan suture zones remain somewhat controversial. The destruction of oceanic basins was also accompanied and followed by: 1) Cretaceous to Early Palaeocene arc magmatism (e. g. Pontide Arc [4–6]); 2) development of accretionary-type fore-arc basins (e. g. Haymana-Polatli Basin [7]; Tuz Gölü Basin [8]); 3) Late Palaeocene to Miocene and younger post-collisional magmatism [9–12]; 4) the development of several blue schist belts (e. g. Late Cretaceous Tavşanlı Zone in Turkey [13]); Çamlıca metamorphic belt in northwestern Turkey [14]; Eocene-Oligocene Cycladic blue schist belt in the central Aegean [15–17]; Lycian Nappes and Menderes Massif [18; 19]; Bolkar Mountains in the Central Taurides [20]; 5) high-grade to low-grade metamorphism affecting larger areas. The nappe translation and burial of large areas beneath advancing ophiolite nappes has resulted in regional metamorphism and consequent formation of crustal-scale metamorphic massifs, such as the Rhodope, Stranja, Cycladic, Menderes massifs and Central Anatolian Crystalline Complex [21–24] (fig. 1).

The Northern Central and East Anatolian faults split the considered region into different crustal blocks and their tectonic regime changes from compressional to a combination of extension and compression. High seismicity is observed within the country and a frequent hot springs related to these tectonic features are widely spread. According to estimates tectonic movements along the North Anatolian Fault, shearing Pontides from the Central Anatolian Plate can reach 20–25 millimetres per year. It results from the general movement of the Arabian and African plates and their pressure to Eurasia. Main directions of these movements are shown in fig. 1. It results in many earthquakes mainly within the Anatolian Plate, including hazardous ones, especially in the northwestern Turkey.

The Black Sea Basin. This basin is a deep depression belonging to the Alpine folded belt. The total thickness of Cretaceous-Quaternary sediments in the central part is estimated to be 14–18 km [25]. The Alpine orogenic belts: Crimea, Greater Caucasus, Pontides, Rhodope-Stranja Massif, Eastern Srednegorie, North Dobrogea and older tectonic units of different origins and ages such as the East European Craton, Moesian Platform, Istanbul Zone and Adzhar-Trialet folded system surround the Black Sea (fig. 2). The Black Sea geology plays its key role in understanding the tectonic evolution of the middle Tethyan Realm, as well as its hydrocarbon potential.

The Black Sea Basin includes two deep sub-basins (the Western Black Sea Basin and the Eastern Black Sea Basin) [26]. They are separated by the mid-Black Sea (Andrusov) Ridge, which is a northwestern stretched basement uplift. The Black Sea is widely recognized as a back-arc basin, but details of its origin and evolution are still a matter of debates [27–31]. Main questions on the history of this lithospheric block are the age of opening of the Black Sea and the configuration of the original Neotethyan fragments in relation to the tectonic development of the region. Concerning the relative age of the Western and Eastern Black Sea basins, there is a growing evidence in recent years of an earlier origin for the former one [31–34]. The present-day subsurface information of the Black Sea was based on tectonostratigraphic studies of the sedimentary infill, sparse

deep seismic sounding (DSS) surveys keeping in mind geologic observations in adjacent land areas [27; 28; 31; 35; 36]. Seismic and gravity data show that the crust shallows to 19 and 22 km depths in the Western and Eastern Black Sea basins, respectively [37]. Geologic subdivision of the Black Sea Basin including Crimea and southern part of the East European Craton is shown in fig. 2.

Mountains of Crimea are a part of the Alpine-Himalayan folding located in south of the plain part of the peninsula, which represents a part of the Scythian Platform. The southern slope of the mountain Crimea is traced below the Black Sea waters in result of young tectonic movements. It is composed of dislocated Triassic-Jurassic flysch deposits and Upper Jurassic carbonate sandy-clayish carboniferous, Paleogene and Neogene rocks. The recorded movements along faults result in earthquakes. The vast territory to the north of the Black Sea is the adjacent East European Craton. The folded system of Greater Caucasus and Adzhar-Trialet system adjoin the Black Sea in the east.

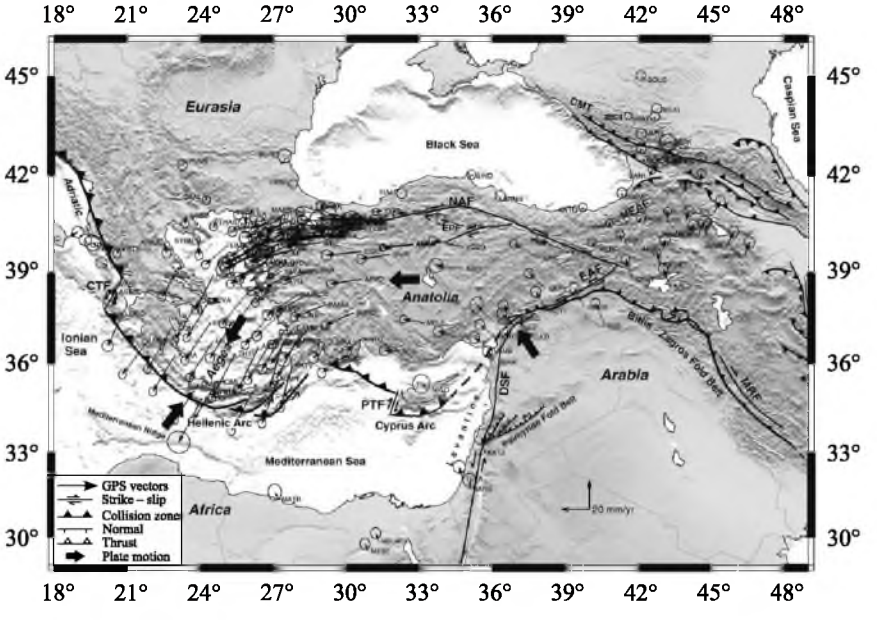

Fig. 1. GPS horizontal velocities and their 95 % confidence ellipses in the Eurasia-fixed reference frame for the period 1988–1997 superimposed on a shaded relief map derived from the GTOPO-30 Global Topography Data taken after the USGS. Bathymetry data are derived from GEBCO/97–BODC, provided by [38–40]. Large arrows designate generalized relative motions of plates with respect to Eurasia (in millimetres per year) (recompiled after [41]). Abbreviations: NAF – North Anatolian Fault; EAF – East Anatolian Fault; DSF – Dead Sea Fault; NEAF – North East Anatolian Fault; EPF – Ezinepazari Fault; CTF – Cephalonia Transform Fault; PTF – Paphos Transform Fault; CMT – Main Caucasus Thrust; MRF – Main Recent Fault

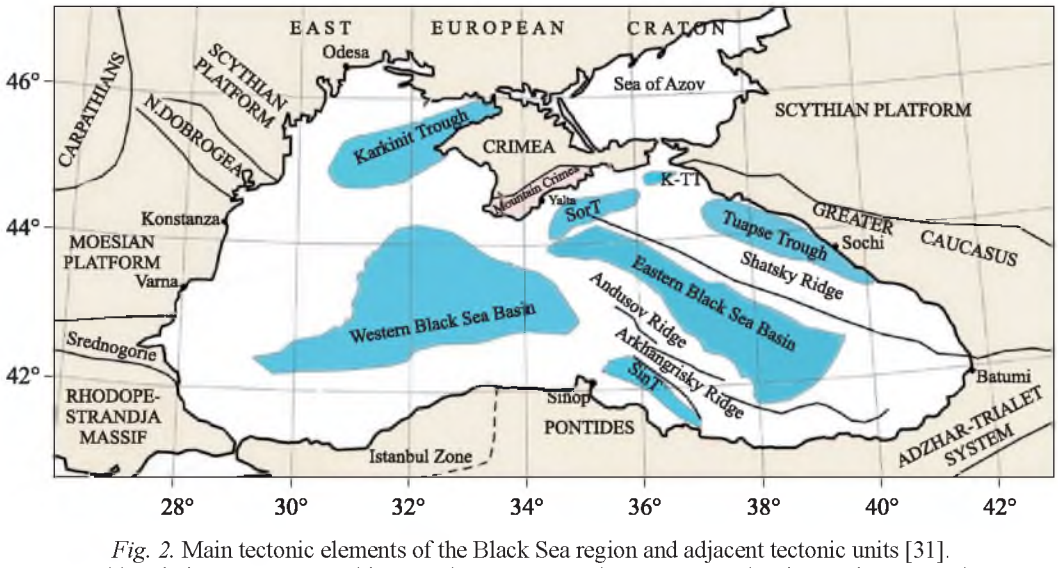

Fig. 2. Main tectonic elements of the Black Sea region and adjacent tectonic units [31]. Abbreviations: SorT – Sorokin Trough; K-TT – Kerch-Taman Trough; SinT – Sinop Trough

Available heat flow data within the region

Eastern Mediterranean Sea and Cyprus. Cyprus in the northeastern part of the Mediterranean Sea is located in between the Anatolian platform to the north and the African Shield to the south. P. Morgan published 33 individual values of heat flow for wells from Cyprus [42; 43]. Results are based on in-hole measurements of the temperature gradient, carried out with a thermistor probe in the conjunction with Wheatstone bridge. Thermal conductivity was obtained from measurements carried out on core- and rock-fragment specimens. The database ranges from as low as six till 46 mW/m^2. After omitting of very low values, the average heat flow of remaining 18 observations was less than 30 mW/m^2. They are comparable to heat flow data from the Eastern Mediterranean, where A. Erickson [44] also reported a vast area of rather low heat flow. Several approaches to explain such low values (rapid sedimentation, low content of radioactive isotopes in the crust, downward water circulation) were discussed. They still did not explain adequately the reason for the low heat flow within an extensive area, spreading over the whole basin of the Mediterranean east of Crete (Levantine Sea), Cyprus, and northern Egypt.

The average of the marine heat flow measurements in the Levantine Sea is (25.7 ± 8.4) mW/m^2 and according to [45] the average from 40 heat flow sites is (47 ± 27) and (39 ± 6) mW/m^2 near Cyprus. On Cyprus, it is (28.0 ± 8.0) mW/m^2. The estimated heat flow in northern Egypt ranges from (38.3 ± 7.0) to (49.9 ± 9.3) mW/m^2, apparently with no consistent trend. To the east, on the coast of Israel, heat flow values increase, ranging from (36.6 ± 22.4) to (56.7 ± 14.2) mW/m^2 along a SSE trend [46]. It apparently correlates with an increase in crustal thickness, which is about 23 km at the northwestern base of the Nile-Delta cone, and close to 40 km beneath Israel.

The marine heat flow data presented by [44] are shown in heat flow density histograms (fig. 3). Their locations are spaced rather uniformly throughout the Eastern Mediterranean. The thermal gradient data were obtained using the Ewing thermograd described in [47]. The penetrations achieved with the piston corer varied between 2.5 and 13.5 m. Thermal conductivity was measured on sediment samples obtained using the needle-probe technique [48] at the same locations as the thermal gradient measurements were fulfilled. The observed data were corrected for an estimated rate of sedimentation of 4.3 cm per 1000 years. The histogram of heat flow density for Cyprus is shown in fig. 4.

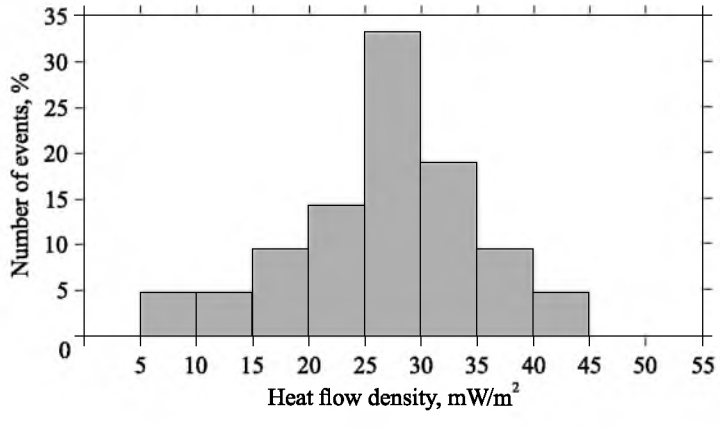

Fig. 3. Heat flow density histogram for the Eastern Mediterranean

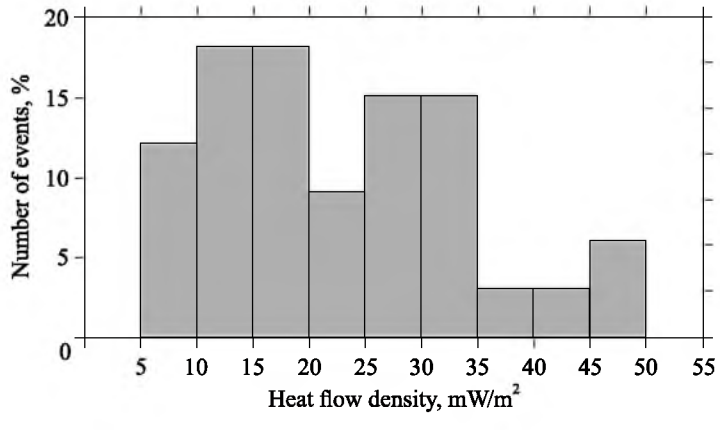

Fig. 4. Heat flow density histogram for Cyprus

Heat flow data from Turkey. The territory of Turkey belongs to the Alpine-Himalayan Belt of orogenesis with significant neotectonic activity, which influences the observable and contrast heat flow. Heat flow determinations were fulfilled on the basis of geothermally studied boreholes. Both temperature logs and rock heat conductivity measurements were used to determine its density. Many boreholes with recorded thermograms have depths not exceeding 200 m, and a ground water circulation, influencing the recorded thermal profiles, had to be taken into account. Conductive heat flow density was calculated considering possible convective effects due to vertical water movements.

A summary of available heat flow determinations for the territory of Turkey were published in [46]. Individual values have a wide range of their changeability from 10–12 until 200 and even 696 mW/m^2 (fig. 5). Very high heat flow was observed in the proximity of active deep faults and zones with extensional tectonic regime in the Marmara Sea, western and southwestern Turkey [49]. The maximum of heat flow observation falls into the interval of 55–75 mW/m^2. A long trailing tail with heat flow exceeding 100 mW/m^2 exists in the right part of the histogram.

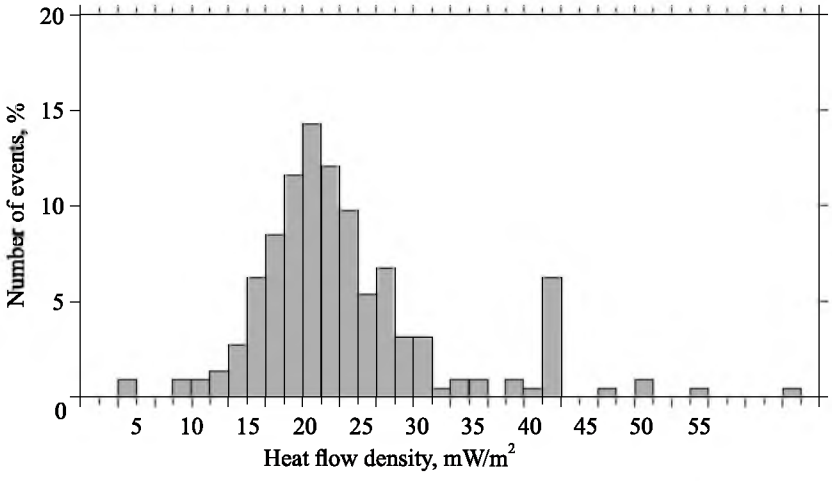

Fig. 5. Heat flow density histogram for Turkey

Heat flow data of the Black Sea. Heat flow studies within the Black Sea were undertaken since the end of sixties and beginning of seventies of the last century. The summary of the most detailed catalogue of available heat flow data exceeding 400 entries was published in 1991 [46]. Around 1/3 values were reported for the eastern Black Sea Basin. Areal distribution of available heat flow observations are shown in fig. 6.

Figure 6 shows that low heat flow density dominates in the Black Sea when comparing its onshore data from countries adjacent the Black Sea Basin. Histograms of its distribution for the Western Black Sea Basin (around 250 individual stations) is shown in fig. 7. The majority of observations exhibits heat flow density, which ranges from 25 until 50 mW/m^2. This diagram shows close to the normal heat flow distributions complicated by its right side with higher values above 60 mW/m^2, observed in the southwestern corner of the sea near shores of Bulgaria. Several heat flow stations within this sector show even higher heat flow up to 80–90 mW/m^2.

As it was mentioned, the number of heat flow stations studied within the Eastern Black Sea Basin is around 100 which is 1/3 of the whole observations fulfilled within the Black Sea. Figure 8 shows in general similar heat flow distribution, but the majority of values are here within the interval of 20–40 mW/m^2, which is lower than ones within the Western Black Sea Basin.

Heat flow map of the studied region

The considered region has a complex geological structure, shown in fig. 1 and 2, where the tectonic regime is changing from compression to extension. Such geologic situation has an imprint on the heat flow distribution within the studied region. Heat flow data reported by a number of researchers were used to compile the heat flow map (fig. 9). The Black Sea, representing a part of the extended Alpine-Himalayan folded belt, is better studied in heat flow, where more than 400 individual heat flow stations are available. On the contrary, the heat flow density information is absent for the time of compiling the map within parts of territories of Syria, Lebanon and Iraq in frames of the map. The heat flow within the whole area is changing in a wide range from as low as ca 20 mW/m^2, typical for the eastern Mediterranean and Cyprus, until more than 100–200 mW/m^2 within the western part of Turkey and adjoining Marmara and Aegean seas. Relatively dense net of heat flow observations exists within the Stavropol Uplift (Ciscaucasia), to the northern areas

of the Greater Caucasus and partly within the southern Ukraine. Many oil exploration wells were studied in heat flow within territories of Romania, Bulgaria and European part of Turkey.

The majority of heat flow data, especially within the Western Black Sea Basin, were received in the period of seventies – nineties of the last century by Soviet researchers [28; 50; 51], they used different marine heat flow probes. Typically, the heat conductivity was measured in situ after the probe penetrated into loose bottom sediments and the necessary time was elapsed to dissipate the friction heat, produced by its insertion.

Within its right lower corner, where heat flow data is absent, it was shown by the oval. This part of the map have to be revised in future after new heat flow data will be accumulated.

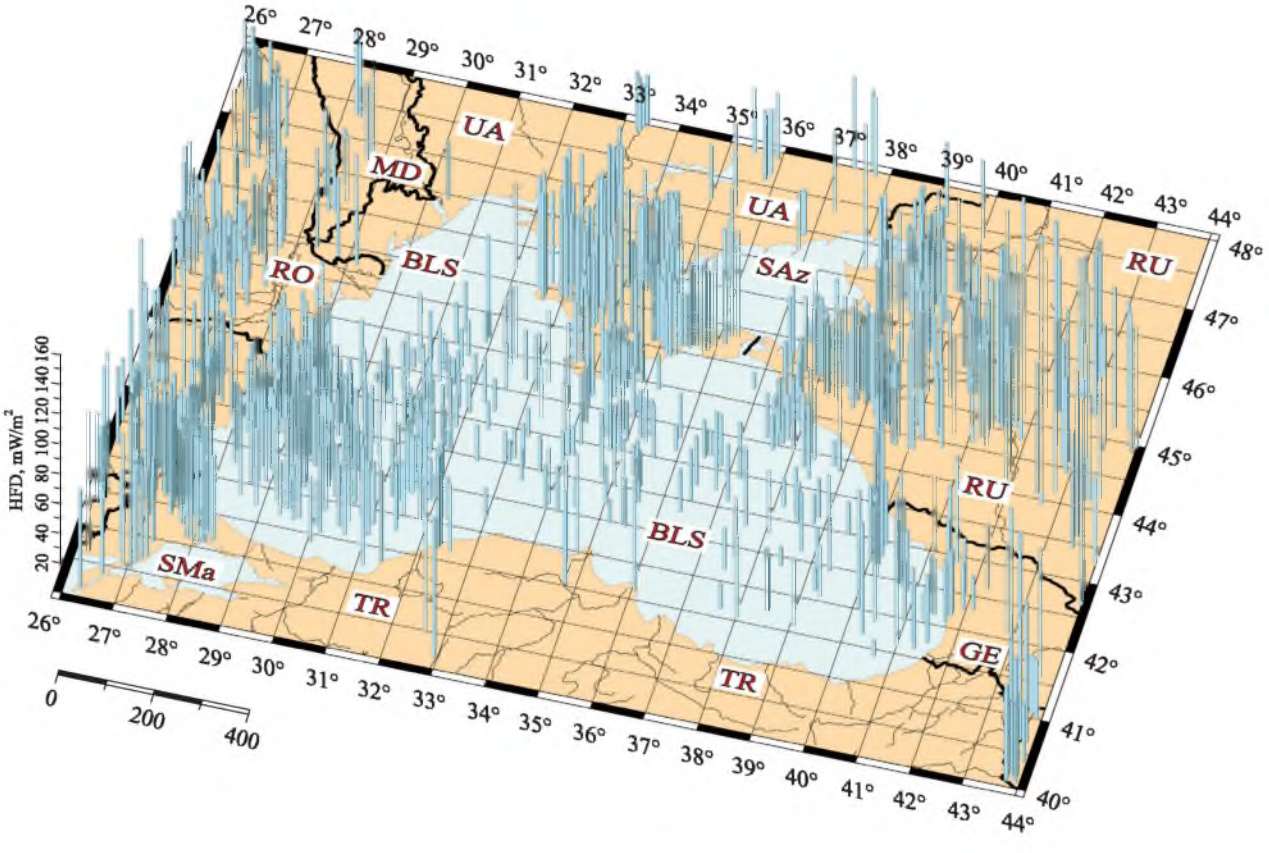

Fig. 6. Positions of marine heat flow stations and adjacent geothermally studied onshore boreholes.
Abbreviations: BLS – Black Sea; SAz – Sea of Azov; SMa – Sea of Marmara;
GE – Georgia; MD – Moldova; RO – Romania; RU – Russia; TR – Turkey; UA – Ukraine

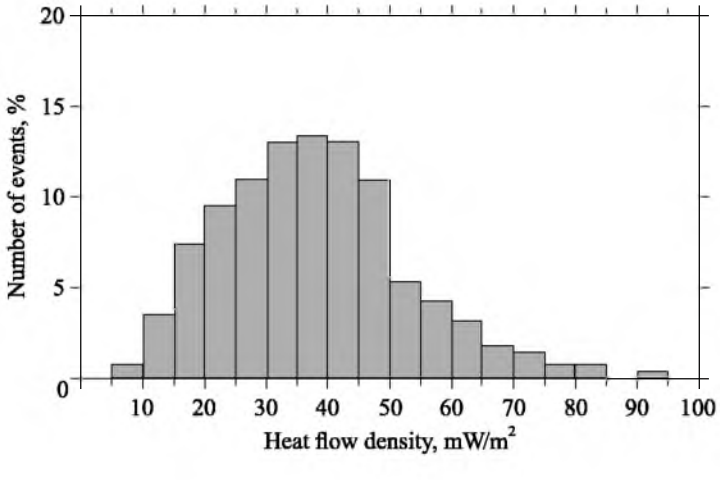

Fig. 7. Heat flow density histogram for the Western Black Sea Basin

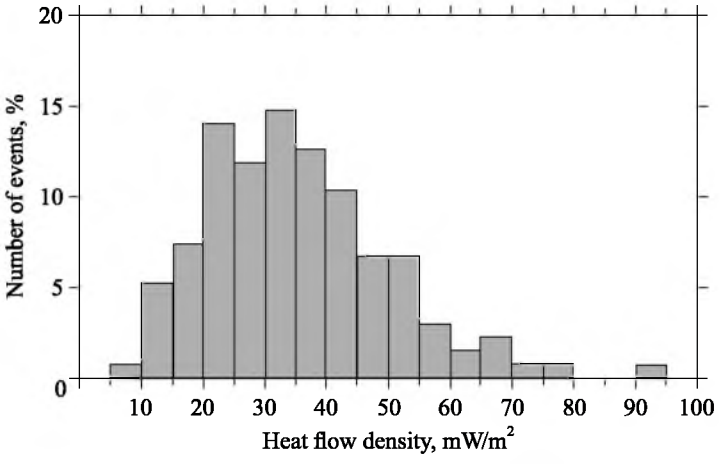

Fig. 8. Heat flow density histogram for the Eastern Black Sea Basin

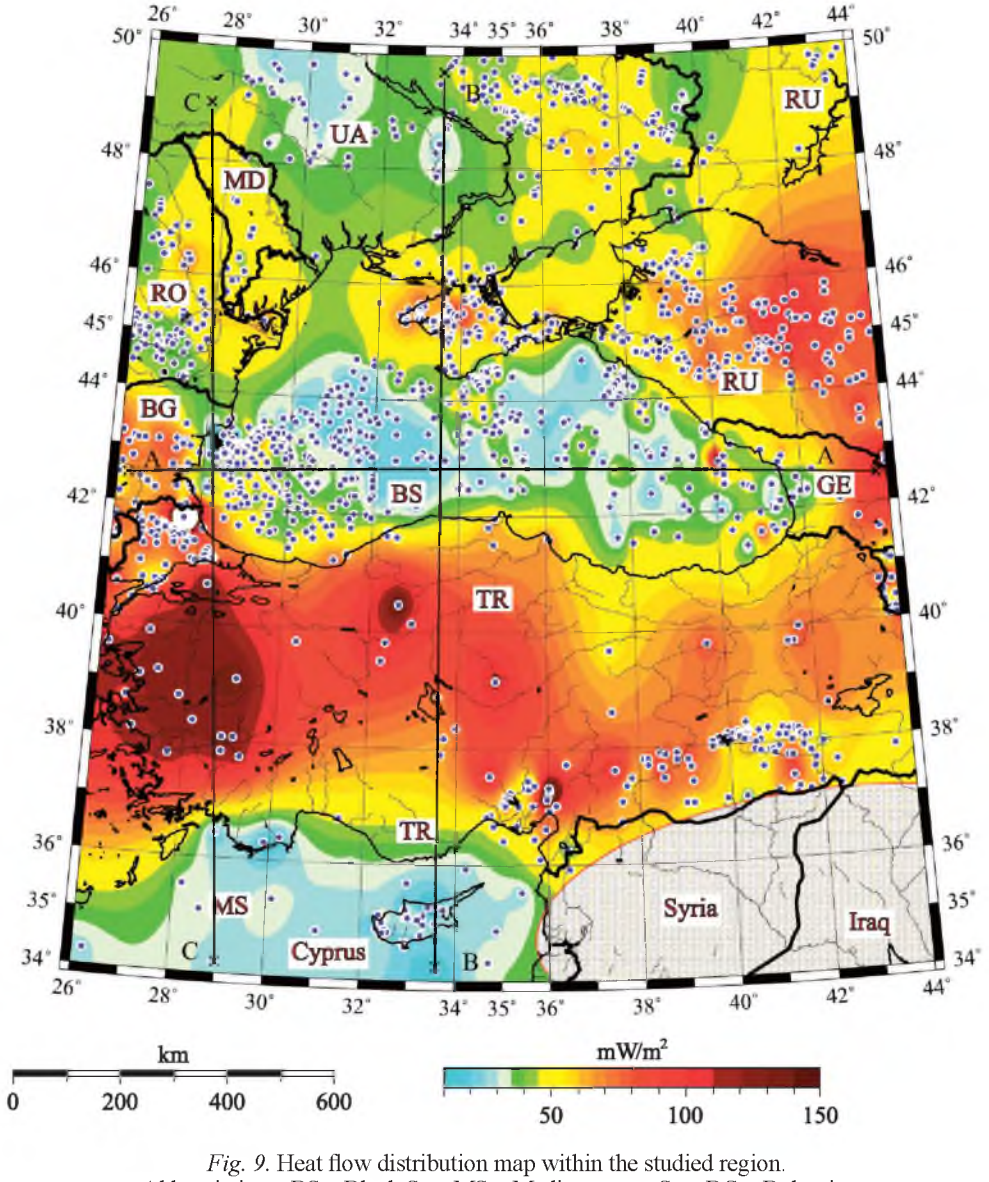

Fig. 9. Heat flow distribution map within the studied region.
Abbreviations: BS – Black Sea; MS – Mediterranean Sea; BG – Bulgaria;
GE – Georgia; MD – Moldova; RO – Romania; RU – Russia; TR – Turkey; UA – Ukraine

Both the Eastern Mediterranean including Cyprus and the Black Sea are characterized in general by relatively low heat flow as it was shown in respective histograms (fig. 3, 4, 7 and 8). High heat flow areas correspond to the territories of Turkey, Greater Caucasus and Ciscaucasia (in particular the Stavropol Uplift, Russia). Geologic structures in the western Turkey exhibit the highest heat flow observed within the whole region.

The general tendency of its variations within the whole map could be noted as its gradual decrease from tectonic structures of the Alpine-Himalayan Belt to the old crustal blocks forming the East European Platform within southern Ukraine in frames of the map. The relatively young Black Sea Basin within this belt represents an exclusion from this general tendency.

Discussion

The Black Sea Basin is the best studied geologic structure in heat flow within the whole considered region. It represents a deep depression within the central part of the Alpine Folded Belt. It was believed that the total thickness of Cretaceous-Quaternary sediments within this basin reaches 14–18 km. At this background the crustal thickness here is reduced to 22–28 km [29; 52], which is typical for young crustal blocks with high heat flow, for instance oil-bearing Pannonian Basin [53].

As it was mentioned above, the Black Sea Depression has generally low heat flow, such heat flow values are observed in the parts of the basin within the maximal sedimentary thickness. The lowest (less 30 mW/m^2) values have been recorded in central parts of the Western and Eastern Black Sea basins. They are separated by a relatively high (40–60 mW/m^2) heat flow zone striking along the western flank of the Andrusov Ridge. The field morphology is different in the West and East Black Sea basins. Higher values are observed on the periphery. They are, as a rule, continuations of anomalous zones from the continent.

The West Basin field is more uniform. In the East Basin, the thermal field is more differentiated. Several high heat flow anomalies mainly of northeastern orientation are distinguished here. Some of them elongated northwestwards cut the main tectonic structures. A series of limited low (20–30 mW/m^2) heat flow anomalies are observed along the Crimean and Caucasian shores. They coincide with zones of deep basement subduction in the offshore troughs (Sorokin and Kerch-Taman ones).

Observed heat flow values of sedimentary basins are influenced by many factors. The most significant one is the sedimentation. Many attempts have been made to calculate the sediment accumulation effect in the Black Sea [28; 51; 54–56].

An erosion from surrounded the Black Sea mountains resulted in delivering to the sea terrigenous material which created accumulating thick sediments at its bottom, blanketing the heat from below. In result, researches observe rather low geothermal gradient within upper parts of loose sediments, hence a low recorded heat flow. This sedimentary thickness is warming up gradually and in future geothermal gradients and heat flow density will become considerably higher. Results of computer modeling show that only the mantle heat flow within the central part of the depression is around 35–40 mW/m^2 [29].

The Crimean Peninsula is far outstanding into the Black Sea. Many heat flow determinations were fulfilled based on temperature-depth profiles of boreholes and heat conductivities of rocks measured in laboratory conditions. In the relatively small territory of the Crimean Peninsula, the interaction of tectonic regions of different origin, structure and evolution has been observed. Almost all major structures of the Earth's crust are represented here: the southern slope of the ancient East European Platform, a part of the Epipaleozoic Scythian Plate, a part of the Alpine-Himalayan Folded System. It is represented by the Crimean mega-anticline bordered by the Indolo-Kuban Edge Sag and a region of the bathypelagic depression of the Black Sea.

The southern part of the Ukraine within frames of the heat flow density map (see fig. 9) includes the Scythian Platform and the Ukrainian Shield, which belong to the Precambrian East European Craton. Geothermal studies on the territories of Ukraine have been under way for a number of years [57; 58]. Thermograms from oil and water wells, as well as ones from ore deposits were used for heat flow determinations. The heat flow values were largely calculated based on the average geothermal gradient and heat conductivity of rock samples. The geothermal gradient varies within this area from 17 (for shallow depth intervals) to 60 mK/m in deep depressions. In several sites within southern Ukraine, the heat flow was determined based on the results of high-precision temperature measurements in shallow boreholes including water wells.

The vast heat flow anomaly within the territory of Turkey was observed in the western and southwestern parts of the country. As it was mentioned above, the tectonic regime within the Anatolian Plate changes from compressional to extensional one in result of the Arabian Plate movement northward and its collision with Eurasia. Main directions of these movements are shown in fig. 10.

Terrestrial surface heat flow density varies regionally from 35 to 115 mW/m^2, with a mean value around 60–70 mW/m^2 (see fig. 5). The fig. 10 shows that the extensional tectonics of the region of western Turkey, south of the Marmara and Aegean seas is characterized by higher heat flow density. These areas are subjected to extensional tectonic regime with many active deep faults, which represent ways of heat supply from deep

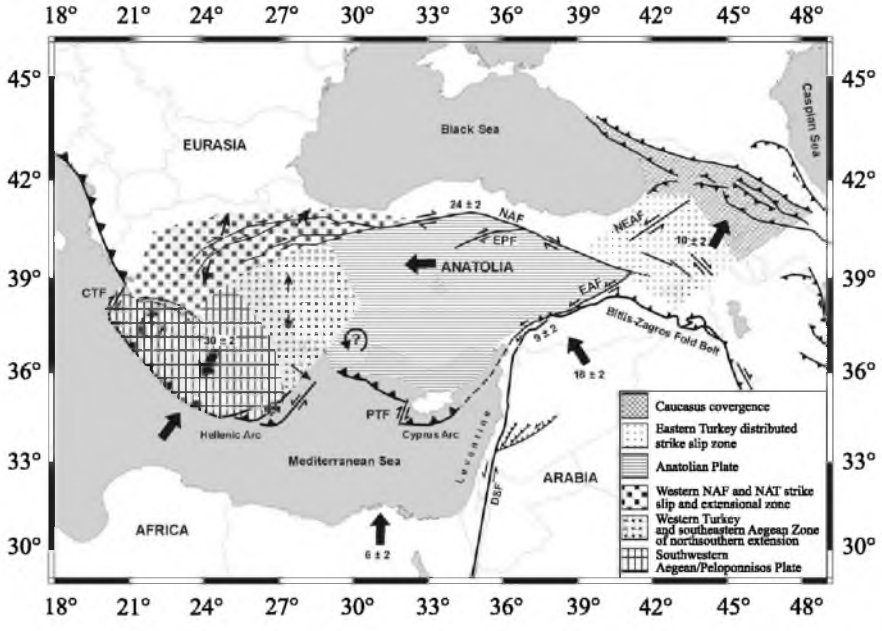

Fig. 10. Schematic map of the principal tectonic settings in the eastern Mediterranean.
Hatching shows areas of coherent motion and zones of distributed deformation.
Large arrows designate generalized regional motion (in millimeters per year) and errors (recompiled after [59; 60]).
Abbreviations: EAF – East Anatolia Fault; DSF – Dead Sea Fault; NAF – North Anatolian Fault;
NEAF – North East Anatolian Fault; CTF – Cephalonia Transform Fault;
PTF – Paphos Transform Fault; MRF – Main Recent Fault; EPF – East Pontides Fault

horizons to the surface. Hence, the high heat flow anomaly is partly caused by the convective mechanism of heat transfer. Fractures create paths for atmospheric water to penetrate to deep horizons where it is heated from hot rocks and forms water steam reservoirs (fig. 11). For instance, one of them the Balcova geothermal system is located at the active Izmir Fault where higher than normal heat flow (110 mW/m^2) was observed.

The natural water steam is used at a few power stations producing «geothermal» electricity, for instance in Kizildere. Regions with low tectonic activity such as parts of European Turkey or regions with compressional and translational tectonics have an average or slightly higher heat flow values.

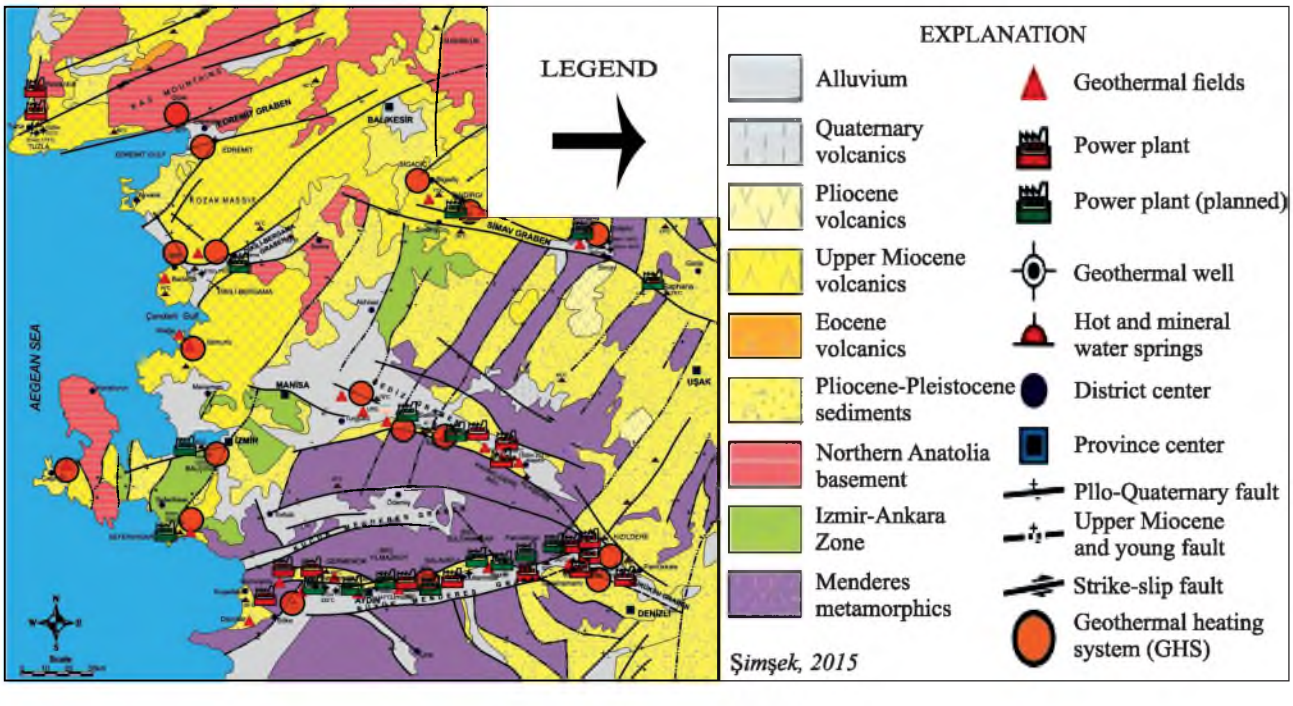

Fig. 11. Geothermal fields and heating systems are related
to a number of active faults in the southwestern Turkey.
Source: [61; 62], modified

In Turkey more than 230 geothermal fields were identified by MTA (General Directorate of Mineral Research and Exploration of Turkey)[1], which can be useful at the economic scale and there are about 2000 hot and mineral water sources (springs, well discharges) with temperatures ranging from 20 to 287 °C. These manifestations are located mainly along the major grabens (such as Buyuk Menderes, Gediz, Dikili-Bergama, Kucuk Menderes, Edremit) along the northern Anatolian Fault Zone and in the Central and Western Anatolia volcanic regions (see fig. 11). Up to now, 1441 geothermal exploratory, production and reinjection wells have been drilled in Turkey in total by the MTA and the private sector [61; 62]. Until the end of 2015, MTA has tendered 142 geothermal fields (including wells) to private sector. The geothermal potential is estimated as 31 500 MW_t up to 2010. Moreover, the updated calculations regarding the geothermal heat capacity potential of Turkey is concentrated at 60 000 MW_t geothermal heat potential [63]. The total geothermal theoretical electricity potential of Turkey (hydrothermal, depth 0–3 km) has been calculated as 4500 MW_e [64].

The installed geothermal heat capacity is 3262.3 MW_t for direct use (including heat pumps) and 650 MW_e for power production in Turkey, where the liquid carbon dioxide and dry ice production factories are integrated to the Kizildere and Salavatli power plants with a production capacity of 240 000 tons/year. The total geothermal technical and economic electricity production potential (hydrothermal, depth 0–3 km) has been calculated as 2000 MW_e (16 billion kilowatt-hour per year) with the additional incentive for 15–20 years by 15 USD cents per kilowatt-hour.

The thermal regime of Cyprus, as mentioned above, is characterized by low heat flow less than 30 mW/m^2, at the same time comparable heat flow values were observed for the Eastern Mediterranean where A. Erickson [44] also reported a vast area of rather low heat flow.

Three profiles: latitudinal A – A, and longitudinal B – B and C – C of the heat flow density variation within the region are shown in fig. 12–14. Their positions are shown in fig. 9. Along the A – A profile, crossing the whole Black Sea Basin and adjacent on land territories there are many heat flow observations. Here the heat flow varies considerably along the whole profile from around 60 in the territory of Bulgaria until 20–30 mW/m^2 within the eastern Black Sea Basin. It clearly shows the increasing heat flow in the Western Black Sea Basin relatively to its eastern part.

Two meridional profiles B – B and C – C show more contrast heat flow variations from 20 until almost 90 mW/m^2 for the profile B – B with rather smooth heat flow increase from the Mediterranean Sea to the central Turkey followed by its decrease to 25 mW/m^2 within the southern part of the East European Craton, where exists a smoother pattern of HFD variations (fig. 13). Its shape depends partly on the observed heat flow within the Black Sea, western Crimea, and heat flow data within Precambrian crustal blocks of the southern Ukraine.

The profile C – C reflects rapid heat flow changes in the meridional direction. It crosses the Mediterranean Sea, the high heat flow anomaly within western Turkey, continues to the eastern Romania through the westernmost part of the Black Sea, and finishes in the western Ukraine (fig. 14).

The profile A – B reflects rapid heat flow changes in the western Turkey direction (fig. 15). Sharp heat flows increase up to 120–140 mW/m^2 is evident in its central part (the western Turkey) (fig. 16) and it crosses tectono-thermally activated crustal blocks, namely the Moesian Plate, North Dobrogea and foredeep of Carpathians, where the heat flow drops to 50–60 mW/m^2. It is even lower in the Western Black Sea Basin (around 20–40 mW/m^2). In all four figures, broken lines show the general trend of heat flow variations along these profiles.

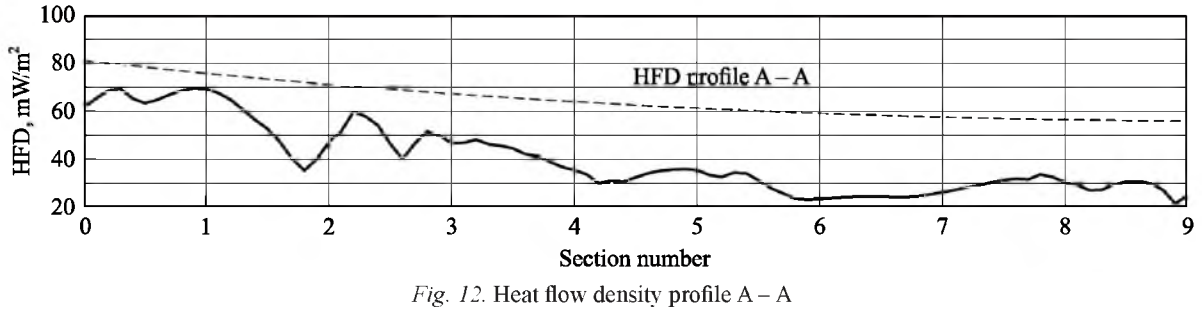

Fig. 12. Heat flow density profile A – A

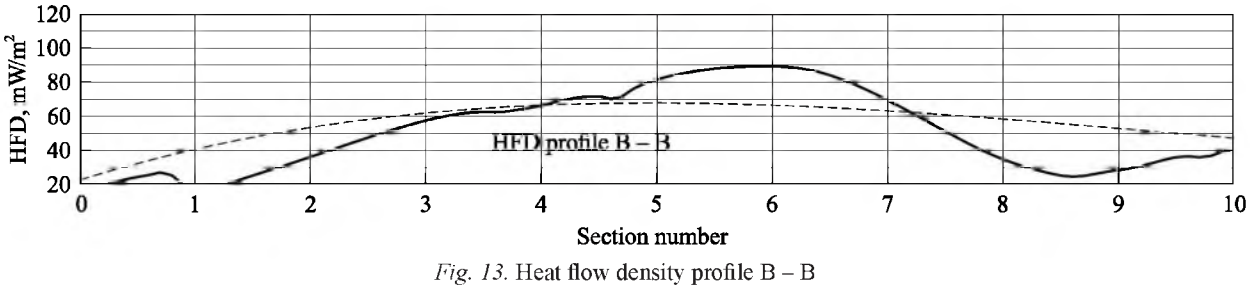

Fig. 13. Heat flow density profile B – B

[1]Mineral Research and Exploration (MTA) of Turkey [Electronic resource]. URL: http://www.mta.gov.tr/eng (date of access: 28.05.2019).

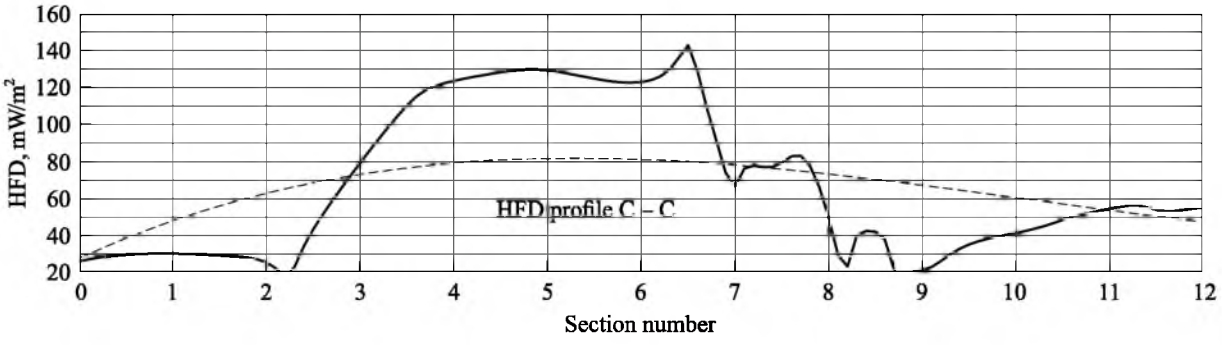

Fig. 14. Heat flow density profile C – C

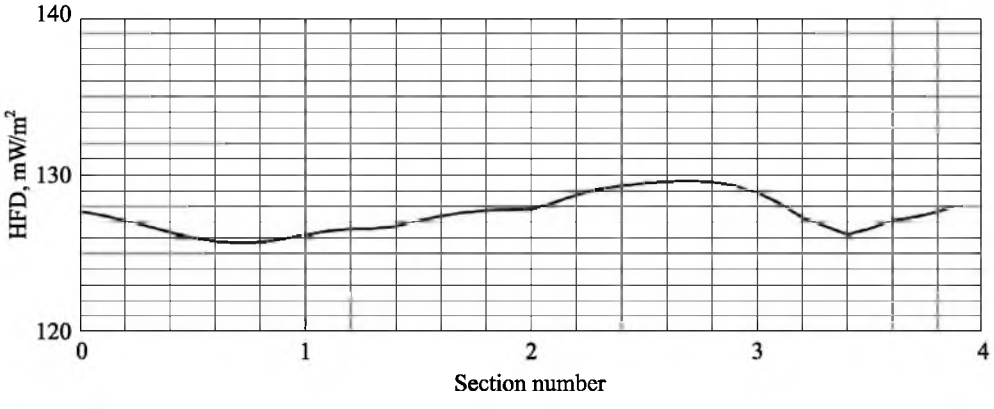

Fig. 15. Heat flow density profile A – B

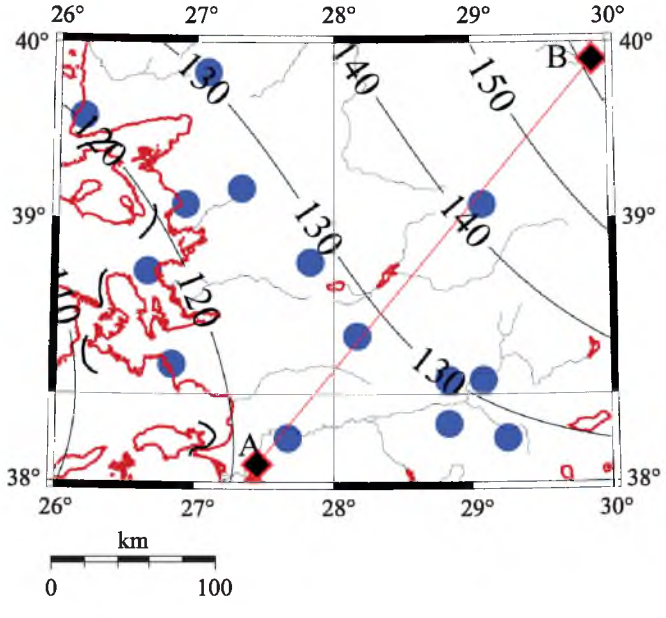

Fig. 16. Western Turkey trend of heat flow density variation:
blue closed circles show locations of boreholes with studied heat flow

Conclusion

A new map of heat flow density distribution was compiled both for the central part of the Alpine-Himalayan Belt including marine areas of the eastern Mediterranean and Black seas, Anatolian Plate, Crimea and adjoining onshore zones of the countries adjacent to the sea: eastern Bulgaria, Romania, Moldova, western Georgia, southern Ukraine, and Russia. The map shows a wide range of heat flow variations from as low as less than 30 and as high as more than 100–150 mW/m^2. The highest anomaly with individual HFD values exceeding

100–140 mW/m^2 exists within the western part of the Anatolian Plate, which belongs to the Alpine crustal folding and evidences the extensional tectonics. Lower values within the region of 20–40 mW/m^2 are typical for the Eastern Mediterranean, Cyprus and the Black Sea Basin. Heat flow data from the Eastern Mediterranean region indicates an extensive area of low heat flow, spreading over the whole basin of the Mediterranean east of Crete (Levantine Sea), Cyprus, and Northern Egypt. The trend apparently correlates with an increase in crustal thickness, which is about 23 km at the northwestern base of the Nile-Delta cone, and close to 40 km beneath Israel. The high heat flow anomaly, observed within the western Turkey, represents young tectono-thermal activated crustal blocks of the Alpine-Himalayan Mobile Belt.

The western Turkey is one of countries rich in geothermal potential within the high heat flow anomaly. Fractured rocks represent ways for deep penetration of atmospheric waters where they are heated by hot rocks and form water steam reservoirs along deep crustal faults. This natural resource of water steam is already used to produce «geothermal» electricity. In result, a significant progress was achieved in Turkey during last decades both in electricity production and in direct use of geothermal energy.

The Black Sea Basin is distinguished by an appreciable minimum in heat flow density (20–40 mW/m^2) when compared to neighboring structures of the Alpine Belt. The observed heat flow decrease is mainly a result of the blanketing effect caused by rapid accumulation of young Pliocene-Quaternary sediments whose thickness reaches several kilometers here according to different estimates. This is clearly confirmed by the dependence of heat flow density on the thickness of sediments of different ages. The heat flow values corrected for the effect of sedimentation are 45–55 mW/m^2. The upper mantle contribution is 35–40 mW/m^2. Nearly the same Moho heat flow values are typical characteristic for the surrounding Alpine-type structures.

Библиографические ссылки

1. Göncüoglu MC, Marroni M, Sayit K, Tekin UK, Ottria G, Pandolfi L, Ellero A. The Ayli Dağ ophiolite sequence (Central-Northern Turkey): a fragment of Middle Jurassic oceanic lithosphere within the Intra-Pontide suture zone. *Ofioliti*. 2012;37(2):77–92.

2. Okay AI, Tüysüz O. Tethyan sutures of northern Turkey. In: Durand B, Jolivet L, Horváth M, Séranne F, editors. *The Mediterranean basin: tertiary extension within the Alpine orogen*. London: Geological Society; 1999. p. 475–515. (Geological Society, London, Special Publications; volume 156).

3. Sengör AMC, Yilmaz Y. Tethyan evolution of Turkey: a plate tectonic approach. *Tectonophysics*. 1981;75:181–241.

4. Okay AI, Şahintürk Ö. Geology of the Eastern Pontides. In: Robinson AG, editor. *Regional and petroleum geology of the Black Sea and surrounding regions*. [S. l.]: Tulsa; 1997. p. 291–311. (AAPG Memoir; 68). DOI: 10.1306/M68612C15.

5. Görür N, Monod O, Okay AI, Sengör AMC, Tüysüz O, Yiğitbas E, et al. Palaeogeographic and tectonic position of the Carboniferous rocks of the western Pontides (Turkey) in frame of the Variscan belt. *Bulletin de la Société Géologique de France*. 1997; 168(2):197–205.

6. Yilmaz Y, Serdar HS, Genc C, Yigitbas E, Gürer ÖF, Elmas A, et al. The geology and evolution of the Tokat Massif, south central Pontides, Turkey. *International Geology Review*. 1997;39(4):365–382. DOI: 10.1080/00206819709465278.

7. Koçyigit A. An example of an accretionary forearc basin from northern Central Anatolia and its implications for the history of subduction of Neo-Tethys in Turkey. *Geological Society of America Bulletin*. 1991;103(1):22–36. DOI: 10.1130/0016-7606(1991)103<0022:AEOAAF>2.3.CO;2.

8. Görür N, Tüysüz O, Sengör AMC. Tectonic evolution of the central Anatolian basins. *International Geology Review*. 1998; 40(9):831–850.

9. Aldanmaza E, Pearcea JA, Thirlwallb MF, Mitchell JG. Petrogenetic evolution of late Cenozoic, post-collision volcanism in western Anatolia, Turkey. *Journal of Volcanology and Geothermal Research*. 2000;102:67–95.

10. Keskin M. Magma generation by slab steepening and breakoff beneath a subduction-accretion complex: an alternative model for collision-related volcanism in Eastern Anatolia, Turkey. *Geophysical Research Letters*. 2003;30(24):8046. DOI: 10.1029/2003GL018019.

11. Boztuğ D, Otlu N, Tatar S. Geological and petrological remarks revealing the differential tectonic uplift in the exhumation history of the collision-related central Anatolian intrusives, Turkey. In: Chatzipetros AA, Pavlides SB, editors. *Proceedings of 5th International Symposium on Eastern Mediterranean Geology; 2004 April 14–20; Thessaloniki, Greece*. [S. l.]: International Symposium on Eastern Mediterranean Geology; 2004. p. 45–48.

12. Altunkaynak S, Dilek Y. Timing and nature of postcollisional volcanism in western Anatolia and geodynamic implications. In: Dilek Y, Pavlides S. *Postcollisional Tectonics and Magmatism in the Mediterranean Region and Asia*. [S. l.]: Geological Society of America; 2006. (Special Paper of the Geological Society of America; volume 409). DOI: 10.1130/2006.2409(17).

13. Okay AI. Tectonic units and sutures in the Pontides, northern Turkey. In: Şengör AMC, editor. *Tectonic Evolution of the Tethyan Region*. Dordrecht: Kluwer Academic Publications; 1989. p. 109–116. (NATO ASI series; volume 259). DOI: https://doi.org/10.1007/978-94-009-2253-2_6.

14. Okay AI, Satir M. Coeval plutonism and metamorphism in a latest Oligocene metamorphic core complex in northwest Turkey. *Geological Magazine*. 2000;137(5):495–516. DOI: 10.1017/S0016756800004532.

15. Altherr R, Schliestedt M, Okrusch M, Seidel E, Kreuzer H, Harre W. Geochronolgy of high pressure rocks on Sifnos (Cyclades, Greece). *Contributions to Mineralogy and Petrology*. 1979;70(3):245–255. DOI: 10.1007/BF00375354.

16. Avigad D, Garfunkel Z. Low-angle faults above and below a blueschist belt – Tinos Island, Cyclades, Greece. *Terra Nova*. 1989;1(2):182–187. DOI: 10.1111/j.1365-3121.1989.tb00350.x.

17. Avigad D, Garfunkel Z. Uplift and exhumation of high-pressure metamorphic terrains: the example of the Cycladic blueschist belt (Aegaen Sea). *Tectonophysics*. 1991;188(3–4):357–372. DOI: 10.1016/0040-1951(91)90464-4.

18. Oberhänsli R, Partzsch JH, Candan O, Çetinkaplan M. First occurrence of Fe-Mg-carpolite documenting a high-pressure metamorphism of the Lycian Nappes, SW Turkey. *International Journal of Earth Sciences.* 2001;89(4):867–873. DOI: 10.1007/s005310000103.

19. Okay AI. Stratigraphic and metamorphic inversions in the central Menderes Massif: a new structural model. *International Journal of Earth Sciences.* 2001;89(4):709–727. DOI: 10.1007/s005310000098.

20. Dilek Y, Whitney DL. Counterclockwise P-T-t trajectory from the metamorphic sole of a Neo-Tethyan ophiolite (Turkey). *Tectonophysics.* 1997;280(3–4):295–310. DOI: 10.1016/S0040-1951(97)00038-3.

21. Şengör AMC, Satir M & Akkörk R. Timing of tectonic events in the Menderes Massif, western Turkey. Implications for tectonic evolution and evidence for Pan-African basement in Turkey. *Tectonics.* 1984;3(7):693–707. DOI: 10.1029/TC003i007p00693.

22. Whitney DL, Dilek Y. Core complex development in Central Anatolia, Turkey. *Geology.* 1997;25(11):1023–1026. DOI: 10.1130/0091-7613(1997)025<1023:CCDICA>2.3.CO;2.

23. Okay AI, Tansel I, Tüysüz O. Obduction, subduction, and collision as reflected in the Upper Cretaceous – Lower Eocene sedimentary record of western Turkey. *Geological Magazine.* 2001;138(2):117–142.

24. Bozkurt E. Extensional *vs* contractional origin for the Southern Menderes Shear Zone, southwest Turkey. Tectonic and metamorphic implications. *Geological Magazine.* 2007;144:191–210.

25. Kutas RI, Kobolev VP, Tsvyashchenko VA. Heat flow and geothermal model of the Black Sea depression. *Tectonophysics.* 1998;291(1–4):91–100. DOI: 10.1016/S0040-1951(98)00033-X.

26. Маловицкий ЮП, Непрочнов ЮП, редакторы. *Структура западной части Черноморского бассейна.* Москва: Наука; 1972. [244 с.].

27. Finetti I, Bricchi G, Del Ben A, Pipan M, Xuan Z. Geophysical study of the Black Sea area. *Bolletino di Geofisica Teorica ed Applicata.* 1988;30:197–324.

28. Okay AI, Sengör AMC, Görur N. Kinematic history of the opening of the Black Sea and its effect on the surrounding regions. *Geology.* 1994;22(3):267–270. DOI: 10.1130/0091-7613(1994)022<0267:KHOTOO>2.3.CO;2.

29. Ustaömer T, Robertson AHF. Tectonic sedimentary evolution of the North Tethyan margin in the central Pontides of Northern Turkey. In: Robinson AG, editor. *Regional and petroleum geology of the Black Sea and surrounding regions.* [S. l.]: Tulsa; 1997. p. 255–290. (AAPG Memoir; 68).

30. Tüysüz O. Geology of the cretaceous sedimentary basins of the Western Pontides. *Geology.* 1999;34(1–2):75–93. DOI: 10.1002/(SICI)1099-1034(199901/06)34:1/2<75::AID-GJ815>3.0.CO;2-S.

31. Hippolyte JC, Müller C, Kaymakci N, Sangu E. Dating of the Black Sea basin: new nannoplankton ages from its inverted margin in the Central Pontides (Turkey). In: Sosson M, Kaymakci N, Stephenson RA, Bergerat F, Starostenko V, editors. *Sedimentary basin tectonics from the Black Sea and Caucasus to the Arabian Platform.* [S. l.]: Geological Society of London; 2010. p. 113–136. (Geological Society, London, Special Publications; volume 340). DOI: http://dx.doi.org/10.1144/SP340.7.

32. Кутас РИ. Анализ термомеханических моделей эволюции осадка Черного моря. *Геофизический журнал.* 2003;25(2):36–47.

33. Khriachtchevskaia O, Stovba S, Stephenson R. Cretaceous – neogene tectonic evolution of the northern margin of the Black Sea from seismic reflection data and tectonic subsidence analysis. In: Sosson M, Kaymakci N, Stephenson RA, Bergerat F, Starostenko V, editors. *Sedimentary basin tectonics from the Black Sea and Caucasus to the Arabian Platform.* [S. l.]: Geological Society of London; 2010. p. 137–157. (Geological Society, London, Special Publications; volume 340). DOI: 10.1144/SP340.8.

34. Stephenson RA, Schellart WP. The Black Sea back-arc: insight to its origin from geodynamical models of modern analogues. In: Sosson M, Kaymakci N, Stephenson RA, Bergerat F, Starostenko V, editors. *Sedimentary basin tectonics from the Black Sea and Caucasus to the Arabian Platform.* [S. l.]: Geological Society of London; 2010. p. 11–21. (Geological Society, London, Special Publications; volume 340). DOI: 10.1144/SP340.2.

35. Neprochnov YP, Kosminskaya IP, Malovitsky YP. Structure of the crust and upper mantle of the Black and Caspian Seas. *Tectonophysics.* 1970;10:517–538.

36. Афанасенков АП, Никишин АМ, Обухов АВ. *Восточно-Черноморский бассейн: геологическое строение и углеводородный потенциал.* Москва: Научный мир; 2007. 172 с.

37. Starostenko V, Buryanov V, Makarenko I, Rusakov O, Stephenson R, Nikishin A, et al. Topography of the crust-mantle boundary beneath the Black Sea Basin. *Tectonophysics.* 2004;381(1–4):211–233.

38. Jones MT, Chairman F, GEBCO Sub-Committee on Digital Bathymetry, editors. User Guide to the GEBCO Digital Atlas and its data sets [Internet; cited 2019 June 14]. [S. l.]: Natural Environment Research Council; 1997. 179 p. Available from: https://www.bodc.ac.uk/projects/data_management/international/gebco/gebco_digital_atlas/gda_development/documents/manual.pdf.

39. Smith WHF, Sandwell DT. Measured and estimated seafloor topography (version 4.2). World Data Centre-A for Marine Geology and Geophysics Research Publication. 1997a. RP-1.

40. Smith WHF, Sandwell DT. Global sea floor topography from satellite altimetry and ship depth soundings. *Science.* 1997;277(5334):1957–1962. DOI: 10.1126/science.277.5334.1956.

41. Любимова ЕА, Никитина ВН, Томара ГА. *Термальные поля внутренних и окраинных морей СССР.* Москва: Наука; 1976. 214 с.

42. Morgan P. Cyprus heat flow with comments on the thermal regime of the Eastern Mediterranean. In: Čermák V, Rybach L, editors. *Terrestrial Heat Flow in Europe.* Berlin: Springer; 1979. p. 144–151. DOI: 10.1007/978-3-642-95357-6_13.

43. Morgan P. Porosity determinations and the thermal conductivity of rock fragments with application to heat flow on Cyprus. *Earth and Planetary Science Letters.* 1975;26:253–262.

44. Erickson AJ. *The measurement and interpretation of heat flow in the Mediterranean and Black Sea* [PhD thesis]. Cambridge: Massachusetts Institute of Technology; 1970.

45. Ryan WBF. *The floor of the Mediterranean Sea* [PhD thesis]. New York: Columbia University; 1969. 196 p.

46. Hurtig E, Haenel R, Zui V, et al. *Geothermal Atlas of Europe.* Gotha: International Association for Seismology and Physics of the Earth's Interior. 1991. 156 p. 36 maps.

47. Langseth MG. Techniques of measuring heat flow through the ocean floor. In: Lee WHK, editor. *Terrestrial Heat Flow in Europe.* Washington: American Geophysical Union; 1965. p. 55–77.

48. Von Herzen RP, Maxwell AE. The measurement of thermal conductivity of deep-sea sediments by a needle-probe method. *Journal of Geophysical Research.* 1959;64:1557–1563.

49. Pfister M, Rybach L, Simsek S. Geothermal reconnaissance of the Marmara Sea region (NW Turkey). Surface heat flow density in an area of active continental extension. *Tectonophysics.* 1998;291(1–4):77–89. DOI: 10.1016/S0040-1951(98)00032-8.

50. Казанцев СА. Разработка и использование технико-методического комплекса: для геотермальных исследований [Интернет; процитировано 5 мая 2016 г.]. Доступно по: http://dlib.rsl.ry/loader/view/01000092000?get=pdf.

51. Кондюрин АБ, Сочельников ВВ. Геотермальное течение в западной части Черного моря. *Океанология.* 1983;23:622–627.

52. Кутас РИ. Геотермальные условия в бассейне Черного моря и его прилегающие районы. *Геофизический журнал.* 2010; 32(6):135–138.

53. Dolton GL. *Pannonian Basin Province, Central Europe (Province 4808) – Petroleum geology, total petroleum systems, and petroleum resource assessment. Bulletin 2204-B.* Reston, Virginia: U. S. Geological Survey; 2006. 47 p.

54. Erickson AJ, von Herzen RE. Downhole temperature measurements and heat flow data in the Black Sea – DSDP leg 42B. *DSDP Initial Reports.* 1978;42(part 2):1085–1103. DOI: 10.2973/dsdp.proc.42-2.152.1978.

55. Голмшток АЮ, Золотарев ВГ. Глубинный тепловой поток бассейна Черного моря. *Доклады Академии наук СССР.* 1980; 254:956–959.

56. Кобзарь ВМ. Тепловой поток и блочная структура литосферы Черноморской впадины. *Геофизический журнал.* 1987; 8:90–94.

57. Кутас РИ, Гордиенко ВВ. *Тепловое поле Украины.* Киев: Наукова думка; 1971. 140 с.

58. Гордиенко ВВ, Гордиенко ИВ, Завгородняя ОВ, Усенко ОВ. *Тепловое поле территории Украины.* Киев: Знания; 2002. 170 с.

59. McClusky S, Balassanian S, Barka A, Demir C, Ergintav S, Georgiev I, et al. Global Positioning System constraints on plate kinematics and dynamics in the eastern Mediterranean and Caucasus. *Journal of Geophysical Research.* 2000;105(B3):5695–5719.

60. McClusky S, Reilinger R, Mahmoud S, Ben Sari D, Tealeb A. GPS constraints on Africa (Nubia) and Arabia plate motions. *Geophysical Journal International.* 2003;155:126–138. DOI: 10.1046/j.1365-246X.2003.02023.x.

61. Mertoglu O, Simsek S, Basarir N. Geothermal Country Update Report of Turkey (2010–2015). In: *Proceedings World Geothermal Congress; 2015 April 19–25; Melbourne, Australia.* No. 01046.

62. Simsek S. *Main Geothermal fields of Western Anatolia, Jeotermal Çalışmalar artiyor* Istanbul: Yer Mühendisliği Blt; 2014.

63. Yilmazer S. *Bati Anadolu'nun Olası Jeotermal Potansiyelinin Belirlenmesi, Türkiye 11. Enerji Kongresi.* Izmir: Tepekule Kongre Merkezi; 2009.

64. *TJD. Geothermal Energy Development Report.* Ankara: Turkish Geothermal Association (TJD); 2013.

References

1. Göncüoglu MC, Marroni M, Sayit K, Tekin UK, Ottria G, Pandolfi L, Ellero A. The Ayli Dağ ophiolite sequence (Central-Northern Turkey): a fragment of Middle Jurassic oceanic lithosphere within the Intra-Pontide suture zone. *Ofioliti.* 2012;37(2):77–92.

2. Okay AI, Tüysüz O. Tethyan sutures of northern Turkey. In: Durand B, Jolivet L, Horváth M, Séranne F, editors. *The Mediterranean basin: tertiary extension within the Alpine orogen.* London: Geological Society; 1999. p. 475–515. (Geological Society, London, Special Publications; volume 156).

3. Sengör AMC, Yilmaz Y. Tethyan evolution of Turkey: a plate tectonic approach. *Tectonophysics.* 1981;75:181–241.

4. Okay AI, Şahintürk Ö. Geology of the Eastern Pontides. In: Robinson AG, editor. *Regional and petroleum geology of the Black Sea and surrounding regions.* [S. l.]: Tulsa; 1997. p. 291–311. (AAPG Memoir; 68). DOI: 10.1306/M68612C15.

5. Görür N, Monod O, Okay AI, Sengör AMC, Tüysüz O, Yiğitbas E, et al. Palaeogeographic and tectonic position of the Carboniferous rocks of the western Pontides (Turkey) in frame of the Variscan belt. *Bulletin de la Société Géologique de France.* 1997; 168(2):197–205.

6. Yilmaz Y, Serdar HS, Genc C, Yigitbas E, Gürer ÖF, Elmas A, et al. The geology and evolution of the Tokat Massif, south central Pontides, Turkey. *International Geology Review.* 1997;39(4):365–382. DOI: 10.1080/00206819709465278.

7. Koçyigit A. An example of an accretionary forearc basin from northern Central Anatolia and its implications for the history of subduction of Neo-Tethys in Turkey. *Geological Society of America Bulletin.* 1991;103(1):22–36. DOI: 10.1130/0016-7606(1991)103<0022:AEOAAF>2.3.CO;2.

8. Görür N, Tüysüz O, Sengör AMC. Tectonic evolution of the central Anatolian basins. *International Geology Review.* 1998; 40(9):831–850.

9. Aldanmaza E, Pearcea JA, Thirlwallb MF, Mitchell JG. Petrogenetic evolution of late Cenozoic, post-collision volcanism in western Anatolia, Turkey. *Journal of Volcanology and Geothermal Research.* 2000;102:67–95.

10. Keskin M. Magma generation by slab steepening and breakoff beneath a subduction-accretion complex: an alternative model for collision-related volcanism in Eastern Anatolia, Turkey. *Geophysical Research Letters.* 2003;30(24):8046. DOI: 10.1029/2003GL018019.

11. Boztuğ D, Otlu N, Tatar S. Geological and petrological remarks revealing the differential tectonic uplift in the exhumation history of the collision-related central Anatolian intrusives, Turkey. In: Chatzipetros AA, Pavlides SB, editors. *Proceedings of 5th International Symposium on Eastern Mediterranean Geology; 2004 April 14–20; Thessaloniki, Greece.* [S. l.]: International Symposium on Eastern Mediterranean Geology; 2004. p. 45–48.

12. Altunkaynak S., Dilek Y. Timing and nature of postcollisional volcanism in western Anatolia and geodynamic implications. In: Dilek Y, Pavlides S. *Postcollisional Tectonics and Magmatism in the Mediterranean Region and Asia.* [S. l.]: Geological Society of America; 2006. (Special Paper of the Geological Society of America; volume 409). DOI: 10.1130/2006.2409(17).

13. Okay AI. Tectonic units and sutures in the Pontides, northern Turkey. In: Şengör AMC, editor. *Tectonic Evolution of the Tethyan Region.* Dordrecht: Kluwer Academic Publications; 1989. p. 109–116. (NATO ASI series; volume 259). DOI: https://doi.org/10.1007/978-94-009-2253-2_6.

14. Okay AI, Satir M. Coeval plutonism and metamorphism in a latest Oligocene metamorphic core complex in northwest Turkey. *Geological Magazine.* 2000;137(5):495–516. DOI: 10.1017/S0016756800004532.

15. Altherr R, Schliestedt M, Okrusch M, Seidel E, Kreuzer H, Harre W. Geochronolgy of high pressure rocks on Sifnos (Cyclades, Greece). *Contributions to Mineralogy and Petrology.* 1979;70(3):245–255. DOI: 10.1007/BF00375354.

16. Avigad D, Garfunkel Z. Low-angle faults above and below a blueschist belt – Tinos Island, Cyclades, Greece. *Terra Nova.* 1989;1(2):182–187. DOI: 10.1111/j.1365-3121.1989.tb00350.x.

17. Avigad D, Garfunkel Z. Uplift and exhumation of high-pressure metamorphic terrains: the example of the Cycladic blueschist belt (Aegaen Sea). *Tectonophysics.* 1991;188(3–4):357–372. DOI: 10.1016/0040-1951(91)90464-4.

18. Oberhänsli R, Partzsch JH, Candan O, Çetinkaplan M. First occurrence of Fe-Mg-carpolite documenting a high-pressure metamorphism of the Lycian Nappes, SW Turkey. *International Journal of Earth Sciences.* 2001;89(4):867–873. DOI: 10.1007/s005310000103.

19. Okay AI. Stratigraphic and metamorphic inversions in the central Menderes Massif: a new structural model. *International Journal of Earth Sciences.* 2001;89(4):709–727. DOI: 10.1007/s005310000098.

20. Dilek Y, Whitney DL. Counterclockwise P-T-t trajectory from the metamorphic sole of a Neo-Tethyan ophiolite (Turkey). *Tectonophysics.* 1997;280(3–4):295–310. DOI: 10.1016/S0040-1951(97)00038-3.

21. Şengör AMC, Satir M & Akkörk R. Timing of tectonic events in the Menderes Massif, western Turkey. Implications for tectonic evolution and evidence for Pan-African basement in Turkey. *Tectonics.* 1984;3(7):693–707. DOI: 10.1029/TC003i007p00693.

22. Whitney DL, Dilek Y. Core complex development in Central Anatolia, Turkey. *Geology.* 1997;25(11):1023–1026. DOI: 10.1130/0091-7613(1997)025<1023:CCDICA>2.3.CO;2.

23. Okay AI, Tansel I, Tüysüz O. Obduction, subduction, and collision as reflected in the Upper Cretaceous – Lower Eocene sedimentary record of western Turkey. *Geological Magazine.* 2001;138(2):117–142.

24. Bozkurt E. Extensional vs contractional origin for the Southern Menderes Shear Zone, southwest Turkey. Tectonic and metamorphic implications. *Geological Magazine.* 2007;144:191–210.

25. Kutas RI, Kobolev VP, Tsvyashchenko VA. Heat flow and geothermal model of the Black Sea depression. *Tectonophysics.* 1998;291(1–4):91–100. DOI: 10.1016/S0040-1951(98)00033-X.

26. Malovitsky YP, Neprochnov YP, editors. *Struktura zapadnoi chasti Chernomorskogo basseina* [Structure of the western part of the Black Sea Basin]. Moscow: Nauka; 1972. [244 p.]. Russian.

27. Finetti I, Bricchi G, Del Ben A, Pipan M, Xuan Z. Geophysical study of the Black Sea area. *Bolletino di Geofisica Teorica ed Applicata.* 1988;30:197–324.

28. Okay AI, Sengör AMC, Görür N. Kinematic history of the opening of the Black Sea and its effect on the surrounding regions. *Geology.* 1994;22(3):267–270. DOI: 10.1130/0091-7613(1994)022<0267:KHOTOO>2.3.CO;2.

29. Ustaömer T, Robertson AHF. Tectonic sedimentary evolution of the North Tethyan margin in the central Pontides of Northern Turkey. In: Robinson AG, editor. *Regional and petroleum geology of the Black Sea and surrounding regions.* [S. l.]: Tulsa; 1997. p. 255–290. (AAPG Memoir; 68).

30. Tüysüz O. Geology of the cretaceous sedimentary basins of the Western Pontides. *Geology.* 1999;34(1–2):75–93. DOI: 10.1002/(SICI)1099-1034(199901/06)34:1/2<75::AID-GJ815>3.0.CO;2-S.

31. Hippolyte JC, Müller C, Kaymakci N, Sangu E. Dating of the Black Sea Basin: new nannoplankton ages from its inverted margin in the Central Pontides (Turkey). In: Sosson M, Kaymakci N, Stephenson RA, Bergerat F, Starostenko V, editors. *Sedimentary basin tectonics from the Black Sea and Caucasus to the Arabian Platform.* [S. l.]: Geological Society of London; 2010. p. 113–136. (Geological Society, London, Special Publications; volume 340). DOI: http://dx.doi.org/10.1144/SP340.7.

32. Kutas RI. [Analysis of thermo-mechanic models of the Black Sea sedimentary evolution]. *Geofizicheskii zhurnal.* 2003;25(2):36–47. Russian.

33. Khriachtchevskaia O, Stovba S, Stephenson R. Cretaceous – neogene tectonic evolution of the northern margin of the Black Sea from seismic reflection data and tectonic subsidence analysis. In: Sosson M, Kaymakci N, Stephenson RA, Bergerat F, Starostenko V, editors. *Sedimentary basin tectonics from the Black Sea and Caucasus to the Arabian Platform.* [S. l.]: Geological Society of London; 2010. p. 137–157. (Geological Society, London, Special Publications; volume 340). DOI: 10.1144/SP340.8.

34. Stephenson RA, Schellart WP. The Black Sea back-arc: insight to its origin from geodynamical models of modern analogues. In: Sosson M, Kaymakci N, Stephenson RA, Bergerat F, Starostenko V, editors. *Sedimentary basin tectonics from the Black Sea and Caucasus to the Arabian Platform.* [S. l.]: Geological Society of London; 2010. p. 11–21. (Geological Society, London, Special Publications; volume 340). DOI: 10.1144/SP340.2.

35. Neprochnov YP, Kosminskaya IP, Malovitsky YP. Structure of the crust and upper mantle of the Black and Caspian Seas. *Tectonophysics.* 1970;10:517–538.

36. Afanasenkov AP, Nikishin AM, Obukhov AV. *Vostochno-Chernomorskii bassein: geologicheskoe stroenie i uglevodorodnyi potentsial* [The eastern Black Sea Basin: geological structure and hydrocarbon potential]. Moscow: Nauchnyi mir; 2007. 172 p. Russian.

37. Starostenko V, Buryanov V, Makarenko I, Rusakov O, Stephenson R, Nikishin A, et al. Topography of the crust-mantle boundary beneath the Black Sea Basin. *Tectonophysics.* 2004;381(1–4):211–233.

38. Jones MT, Chairman F, GEBCO Sub-Committee on Digital Bathymetry, editors. User Guide to the GEBCO Digital Atlas and its data sets [Internet; cited 2019 June 14]. [S. l.]: Natural Environment Research Council; 1997. 179 p. Available from: https://www.bodc.ac.uk/projects/data_management/international/gebco/gebco_digital_atlas/gda_development/documents/manual.pdf.

39. Smith WHF, Sandwell DT. Measured and estimated seafloor topography (version 4.2). World Data Centre-A for Marine Geology and Geophysics Research Publication. 1997a. RP-1.

40. Smith WHF, Sandwell DT. Global sea floor topography from satellite altimetry and ship depth soundings. *Science.* 1997;277(5334):1957–1962. DOI: 10.1126/science.277.5334.1956.

41. Lubimova EA, Nikitina VN, Tomara GA. *Termal'nye polya vnutrennikh i okrainnykh morei SSSR* [Thermal fields of inner and marginal seas of the USSR]. Moscow: Nauka; 1976. 214 p. Russian.

42. Morgan P. Cyprus heat flow with comments on the thermal regime of the Eastern Mediterranean. In: Čermák V, Rybach L, editors. *Terrestrial Heat Flow in Europe.* Berlin: Springer; 1979. p. 144–151. DOI: 10.1007/978-3-642-95357-6_13.

43. Morgan P. Porosity determinations and the thermal conductivity of rock fragments with application to heat flow on Cyprus. *Earth and Planetary Science Letters.* 1975;26:253–262.

44. Erickson AJ. *The measurement and interpretation of heat flow in the Mediterranean and Black Sea* [PhD thesis]. Cambridge: Massachusetts Institute of Technology; 1970.

45. Ryan WBF. *The floor of the Mediterranean Sea* [PhD thesis]. New York: Columbia University; 1969. 196 p.

46. Hurtig E, Haenel R, Zui V, et al. *Geothermal Atlas of Europe.* Gotha: International Association for Seismology and Physics of the Earth's Interior. 1991. 156 p. 36 maps.

47. Langseth MG. Techniques of measuring heat flow through the ocean floor. In: Lee WHK, editor. *Terrestrial Heat Flow in Europe.* Washington: American Geophysical Union; 1965. p. 55–77.

48. Von Herzen RP, Maxwell AE. The measurement of thermal conductivity of deep-sea sediments by a needle-probe method. *Journal of Geophysical Research.* 1959;64:1557–1563.

49. Pfister M, Rybach L, Simsek S. Geothermal reconnaissance of the Marmara Sea region (NW Turkey). Surface heat flow density in an area of active continental extension. *Tectonophysics.* 1998;291(1–4):77–89. DOI: 10.1016/S0040-1951(98)00032-8.

50. Kazantsev SA. [Development and utilization of equipment-methodical complex: for geothermal investigations] [Internet; cited 2016 May 5]. Available from: http://dlib.rsl.ry/loader/view/01000092000?get=pdf. Russian.

51. Kondiurin AB, Sochelnikov VV. [Geothermal flow in western part of the Black Sea]. *Okeanologiya.* 1983;23:622–627. Russian.

52. Kutas RI. Geothermal conditions of the Black Sea Basin and its surroundings. *Geofizicheskii zhurnal.* 2010;32(6):135–138. Russian.

53. Dolton GL. *Pannonian Basin Province, Central Europe (Province 4808) – Petroleum geology, total petroleum systems, and petroleum resource assessment. Bulletin 2204-B.* Reston, Virginia: U. S. Geological Survey; 2006. 47 p.

54. Erickson AJ, von Herzen RE. Downhole temperature measurements and heat flow data in the Black Sea – DSDP leg 42B. *DSDP Initial Reports.* 1978;42(part 2):1085–1103. DOI: 10.2973/dsdp.proc.42-2.152.1978.

55. Golmshtok AJ, Zolotarev VG. [Deep-seated heat flow of the Black Sea Basin]. *Doklady Akademii nauk SSSR.* 1980;254: 956–959. Russian.

56. Kobzar VM. [Heat flow and block structure of the lithosphere of the Black Sea depression]. *Geofizicheskii zhurnal.* 1987;8: 90–94. Russian.

57. Kutas RI, Gordienko VV. *Teplovoe pole Ukrainy* [Thermal field of Ukraine]. Kiev: Naukova dumka; 1971. 140 p. Russian.

58. Gordienko VV, Gordienko IV, Zavgorodnyaya OV, Usenko OV. *Teplovoe pole territorii Ukrainy* [Thermal field of the territory of Ukraine]. Kiev: Znanniya; 2002. 170 p. Russian.

59. McClusky S, Balassanian S, Barka A, Demir C, Ergintav S, Georgiev I, et al. Global Positioning System constraints on plate kinematics and dynamics in the eastern Mediterranean and Caucasus. *Journal of Geophysical Research.* 2000;105(B3):5695–5719.

60. McClusky S, Reilinger R, Mahmoud S, Ben Sari D, Tealeb A. GPS constraints on Africa (Nubia) and Arabia plate motions. *Geophysical Journal International.* 2003;155:126–138. DOI: 10.1046/j.1365-246X.2003.02023.x.

61. Mertoglu O, Simsek S, Basarir N. Geothermal Country Update Report of Turkey (2010–2015). In: *Proceedings World Geothermal Congress; 2015 April 19–25; Melbourne, Australia.* No. 01046.

62. Simsek S. *Main Geothermal fields of Western Anatolia, Jeotermal Çalişmalar artiyor* Istanbul: Yer Mühendisliği Blt; 2014.

63. Yilmazer S. *Bati Anadolu'nun Olası Jeotermal Potansiyelinin Belirlenmesi, Türkiye 11. Enerji Kongresi.* Izmir: Tepekule Kongre Merkezi; 2009.

64. *TJD. Geothermal Energy Development Report.* Ankara: Turkish Geothermal Association (TJD); 2013.

Received by editorial board 18.06.2019.